AD-A133 863 STRUCTURE AND PHASE TRANSITIONS IN BROMINE AND POTASSIUM-MERCURY INTERCAL..(U) MASSACHUSETTS INST OF TECH CAMBRIDGE A ERBIL ET AL. APR 83 AFOSR-TR-83-0761 1/1

UNCLASSIFIED F49620-83-C-0011 F/G 7/3 NL

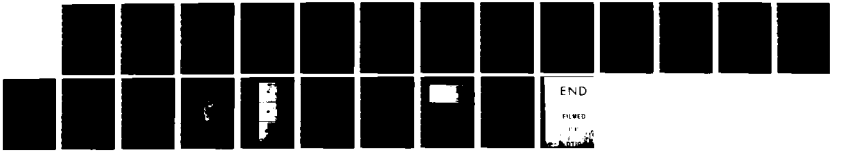

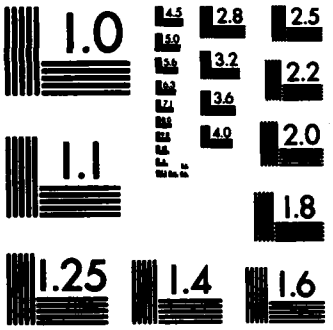

(2)

REPORT DOCUMENTATION PAGE

READ INSTRUCTIONS BEFORE COMPLETING FORM

1. REPORT NUMBER: AFOSR-TR- 83-0761
2. GOVT ACCESSION NO.: AD-A133 863
3. RECIPIENT'S CATALOG NUMBER:

AD-A133 863

4. TITLE (and Subtitle): STRUCTURE AND PHASE TRANSITIONS IN BROMINE AND POTASSIUM-MERCURY INTERCALATED GRAPHITE
5. TYPE OF REPORT & PERIOD COVERED: REPRINT
6. PERFORMING ORG. REPORT NUMBER:

7. AUTHOR(s): A. ERBIL, G. TIMP, A.R. KORTAN, R.J. BIRGENEAU, M.S. DRESSELHAUS

8. CONTRACT OR GRANT NUMBER(s): F49620-83-C-0011

9. PERFORMING ORGANIZATION NAME AND ADDRESS
Massachusetts Institute of Technology
77 Massachusetts Avenue
Cambridge, MA 02139

10. PROGRAM ELEMENT, PROJECT, TASK AREA & WORK UNIT NUMBERS
61102F
2306/C3

11. CONTROLLING OFFICE NAME AND ADDRESS
Air Force Office of Scientific Research/NE
Bolling AFB, DC 20332

12. REPORT DATE: April 1983
13. NUMBER OF PAGES: 19

14. MONITORING AGENCY NAME & ADDRESS(if different from Controlling Office):

15. SECURITY CLASS. (of this report): Unclassified
15a. DECLASSIFICATION/DOWNGRADING SCHEDULE:

16. DISTRIBUTION STATEMENT (of this Report)

Approved for public release; distribution unlimited.

17. DISTRIBUTION STATEMENT (of the abstract entered in Block 20, if different from Report)

18. SUPPLEMENTARY NOTES
Conference Proceedings, May 1983, Synthetic Metals (accepted for publication) pages unknown.

19. KEY WORDS (Continue on reverse side if necessary and identify by block number)
intercalated graphite
structural phase transitions
intercalation kinetics
intercalate domains
anisotropic melting

20. ABSTRACT (Continue on reverse side if necessary and identify by block number)

See Over.

High resolution x-ray scattering and electron microscopy results relevant to the in-plane structure of two prototype graphite intercalation compound (GIC) systems, Br_2-GIC and KHg_x-GIC, are presented. Particular emphasis is given to intercalation kinetics and to structural coherence. Of special interest is the measurement using high resolution x-ray scattering of an intrinsic in-plane intercalate domain size in Br_2-GIC larger than 10,000 Å. Evidence is presented for the formation of a two-dimensional incommensurate domain wall structure for the Br_2 intercalant along the 7-fold direction above T_C = 69.08°C for stage 4 $C_{28}Br_2$. Evidence is also presented in the same compound for two-dimensional anisotropic melting at T_m = 100.25°C. Large dislocation-free regions (100 Å x 500 Å) are observed directly in the lattice fringe images of a stage 1 KHg-GIC sample.

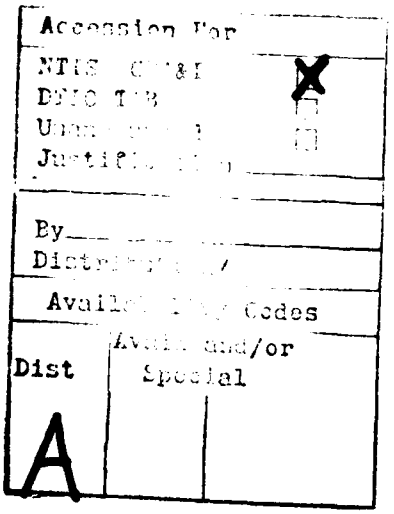

STRUCTURE AND PHASE TRANSITIONS IN BROMINE AND POTASSIUM-MERCURY INTERCALATED GRAPHITE

A. Erbil,*‡ G. Timp,†‡ A. R. Kortan,* R. J. Birgeneau*
and M. S. Dresselhaus†*‡

Massachusetts Institute of Technology
Cambridge, MA 02139

SUMMARY

High resolution x-ray scattering and electron microscopy results relevant to the in-plane structure of two prototype graphite intercalation compound (GIC) systems, Br_2-GIC and KHg_x-GIC, are presented. Particular emphasis is given to intercalation kinetics and to structural coherence. Of special interest is the measurement using high resolution x-ray scattering of an intrinsic in-plane intercalate domain size in Br_2-GIC larger than 10,000 Å. Evidence is presented for the formation of a two-dimensional incommensurate domain wall structure for the Br_2 intercalant along the 7-fold direction above T_C = 69.08°C for stage 4 $C_{28}Br_2$. Evidence is also presented in the same compound for two-dimensional anisotropic melting at T_m = 100.25°C. Large dislocation-free regions (100 Å x 500 Å) are observed directly in the lattice fringe images of a stage 1 KHg-GIC sample.

---

*Department of Physics.

†Department of Electrical Engineering and Computer Science.

‡Center for Materials Science and Engineering.

INTRODUCTION

A detailed knowledge of the structure of the intercalate layer is necessary to specify the electronic and phonon dispersion relations and is therefore of fundamental importance to our understanding of the electronic, transport, magnetic and superconducting properties of graphite intercalation compounds (GIC) [1]. Of the various intercalation compounds that have been studied, only a few are known to exhibit in-plane structures commensurate with the adjacent graphite layers and to have long-range coherence. In this paper we discuss two prototype systems which do exhibit such long-range order, the acceptor Br_2-GIC system, of particular interest because of its novel two-dimensional phase transitions [2,3] and the donor KHg_x-GIC system, of interest because of its superconducting properties [4]. Particular emphasis is given to the intercalation kinetics, and to the structure and structural coherence. Of special interest is the measurement of an intrinsic in-plane intercalate domain size in Br_2-GIC larger than 10,000 Å [2]. Novel 2-dimensional phase transitions are described in the intercalate layer of the Br_2-GIC system.

EXPERIMENTAL DETAILS

The two major techniques used in these structural studies are high resolution x-ray scattering and electron microscopy. To achieve and quantify the long-range in-plane intercalate ordering, it was necessary to use specially selected Kish graphite single crystals. These samples had typical sizes of $2 \times 1 \times 0.1$ mm^3.

For the high resolution x-ray measurements, the samples were intercalated in-situ on the x-ray spectrometer by a vapor transport technique in a pyrex

chamber [2,3]. Two separate two-stage ovens were used to control the temperature of the sample and of the intercalant, independently. The experiments were carried out on a two-axis x-ray spectrometer with the use of Mo $K\alpha$ (λ = 0.7107 Å) radiation from a Rigaku 12-KW rotating anode x-ray source. For most of the measurements, pyrolytic graphite crystals were used as monochromator and analyzer. The longitudinal resolution was 3.3×10^{-2} $Å^{-1}$ half width at half maximum (HWHM) and the transverse in-plane resolution was 2.8×10^{-3} $Å^{-1}$ HWHM at $q = 1.45$ $Å^{-1}$.

For the transmission electron microscopy studies a JEOL 200CX microscope with a high resolution side-entry goniometer stage and a LaB_6 filament was used.[5] The point-to-point resolution was 2.9 Å. Suitably thin regions (1 μm diameter x 100 Å thick) of a foil were first investigated using selected area electron diffraction and diffraction contrast techniques. Following this, the lattice was imaged directly, choosing a minimum number of beams. The typical accelerating voltage was 200 kV and the condenser aperture used was 200 μm in diameter. The micrographs were recorded on Kodak S0163 electron microscopy film with exposure times of about 5 seconds. The micrographs were subsequently analyzed for lattice constants and fringe integrity using an optical diffractometer.

RESULTS FOR Br_2-GIC

It has been known for some time [6] that the Br_2-GIC system has an in-plane intercalate structure commensurate with the adjacent graphite layers, though it is only recently that the room temperature in-plane structure has been identified as a centered ($\sqrt{3} \times 7$) rectangular structure with four Br_2 molecules per 2-D unit cell [2,3,7,8], as shown in Fig. 1. This structure corresponds to an in-plane stoichiometry of $C_{7n}Br_2$, where n is the stage

index. The 7-fold axis is oriented along the [110] direction of the graphite so that there are three equivalent domains. An electron diffraction pattern exhibiting one of these domains is shown in Fig. 2a. This pattern was taken from a residue compound and supports the ($\sqrt{3}$ x 7) rectangular structure implied by the x-ray diffraction results of various workers [2,3,7,8].

As the stage index increases, the interplanar intercalant interaction becomes very small. By stage 4, the Br_2-GIC system exhibits quasi 2D behavior, as is established by the following argument based on x-ray diffraction measurements. Whereas the reciprocal lattice points with contributions from both Br_2 and carbon correspond to true 3-D peaks, the pure Br_2 superlattice points exhibit Bragg rods rather than points at room temperature [3]. The rods, which are oriented in the c-direction, indicate the absence of long range order in this direction. At 300 K the rods show a 30% sinusoidal modulation due to the correlations between nearest intercalate planes. However, by 325 K the modulation vanishes so that at these higher temperatures the Br_2 is essentially 2-D [3].

The disappearance of interlayer intercalate correlation in $C_{28}Br_2$ at 325 K while the in-plane commensurate ordering persists is of particular significance. Previous studies of this phenomenon have been confined to the alkali metal-GIC, where for the high stage compounds (n > 2), it has been reported [1,9-11] that the disappearance of intercalate interlayer correlations occurs at the same temperature that long-range in-plane structural order is lost. The findings in the alkali metal-GIC are thus qualitatively different from those for the case of stage 4 Br_2-GIC, where the in-plane commensurate order is apparently unaffected by the loss of interplanar intercalate correlation. These results indicate the need for a

more general study of the relation between intraplanar and interplanar phase transitions in intercalated graphite, if indeed such a relation exists.

We have investigated the Br(0,6,0) Bragg peak as a function of time to probe the kinetics of Br_2 intercalation into single crystal kish graphite [3]. Scans through the Br(0,6,0) peak position taken at various times after the introduction of Br_2 gas are shown in Fig. 3. After 4 hours, no Bragg peak nor diffuse background appeared, indicating that no intercalation had taken place. However, after 330 minutes, the Bragg peak began to grow very rapidly, indicating the start of intercalation. Figure 4 shows the integrated intensity of the Br(0,6,0) peak as a function of time during the intercalation process. The absence of intensity until t = 330 min. can be interpreted to indicate that either the intercalation process has not yet started or that the intercalated Br_2 molecules are completely disordered in the graphite matrix. Our interpretation of the onset of intercalation is verified by the absence of any observable change in the background scattering, which implies the absence of disordered intercalant. We further note that by t ~ 800 min., the integrated intensity reaches its saturation value. The low background scattering provides evidence that the majority of the intercalated Br_2 molecules form ordered intercalate domains.

Another important feature of Fig. 3 is the observation that the linewidth remains resolution-limited throughout the intercalation process, although the integrated intensity increases with time [3]. This provides evidence that large domain sizes are formed, starting with the initiation of intercalation. Because these experiments were performed with a graphite monochromator and analyzer, we place a lower limit of 2000 Å on the average domain size during intercalation.

The novel features of the intercalation kinetics exhibited by Figs. 3 and 4 bear further comment. These results indicate that under the specified intercalation conditions, the establishment of a stage 4 compound from an unintercalated state occurs on a time scale of less than 2 hours. The linewidth studies indicate that after 6.3 hours of exposure to Br_2, the sample contains regions of unintercalated graphite and regions of stage 4 Br_2-GIC with a large average intercalate domain size. As intercalation proceeds, the stage 4 region grows at the expense of the unintercalated region, until the entire sample is fully intercalated to stage 4. These growth kinetics for vapor phase intercalation in Br_2-GIC are in contrast to the very elegant observations of electrochemical intercalation in the H_2SO_4-GIC system where staging transitions are definitely observed [12]. In the H_2SO_4-GIC studies, an electrochemical potential was used to drive the intercalant into a highly oriented pyrolytic graphite (HOPG) host material and Raman scattering was used for determination of the staging transitions. More detailed study of the intercalation kinetics using x-ray scattering is needed to determine whether the occurrence of $n \leftrightarrow n-1$ staging transitions are related to the intercalant species, the nature of the graphite host material, the nature of the driving force for intercalation, or the intercalation conditions.

For measurement of the intrinsic Br_2 in-plane domain size by x-ray diffraction, germanium (111) crystals were employed as monochromator and analyzer in the W-configuration.[3,13] The resolution function of the non-dispersive configuration was measured using a Si(111) reflection at the sample position. By scaling the measured resolution function to Br_2 superlattice peaks, we show that although the width of the longitudinal scan is resolution-limited, the transverse scan has substantial finite size

broadening, in addition to the linewidth contribution from mosaicity.[3] The finite size contribution to the transverse HWHM of the Br(0,4,0) peak is $< 0.0003\ \text{Å}^{-1}$, which corresponds to an intercalate bromine domain size $> 1\ \mu m$ in the commensurate phase [2,3].

With regard to phase transitions, the Br_2 layers in the stage 4 compound exhibit a particularly interesting commensurate-incommensurate transition at $T_C = 69.084 \pm 0.010°C$ [2,3]. This phase transition can be understood on the basis of the following physical argument. The graphite plane is very rigid and therefore the in-plane unit cell does not change much with varying temperature. The Br_2 plane, on the other hand, is very soft and highly anharmonic. The concomitant difference in thermal expansion causes the Br_2 planes to undergo a commensurate-incommensurate transition with increasing temperature. High resolution x-ray scattering studies clearly demonstrate that in the incommensurate phase, the Br_2 molecules predominantly occupy commensurate sites with the thermal expansion being accomodated by shifts from one sublattice to another in the 7-fold direction. This, in turn, means that the commensurate-incommensurate transition and the incommensurate phase in general should be well-described by a domain wall model [3].

A detailed theory for a 1D commensurate-incommensurate transition in a 2D lattice has been given by Pokrovsky and Talapov [14]. They predict that the domain wall density and hence the incommensurability should initially rise as $(T-T_C)^{1/2}$ but should saturate as the domain wall density increases. We observe just this behavior [2,3], with an exponent of 0.50 ± 0.02. It is found, in addition, that the incommensurate peak position and intensities are well described by a sharp domain wall model with domain wall widths less than

one unit cell and with a displacement at the walls of 2b/7, where b is the lattice constant in the 7-fold direction [2,3].

Corroborating evidence for the commensurate-incommensurate phase transition in the Br_2-GIC system has come from analysis of the temperature dependence of the lineshape, linewidth and intensity of the bromine molecular stretch mode in the Raman spectra [15]. Additional evidence for this phase transition is provided by the sequence of electron diffraction patterns shown in Fig. 2 for several temperatures close to T_C. Starting at room temperature with the commensurate ($\sqrt{3}$ x 7) superlattice in Fig. 2a, raising the temperature above T_C causes formation of a double diffraction pattern along the 7-fold direction but not along the $\sqrt{3}$-fold direction, as shown in Fig. 2b for T = 72°C. The formation of this double diffraction pattern is consistent with a transition to an incommensurate phase with domain walls, as indicated by the x-ray results discussed above.

The Br_2 layers further exhibit a particularly unusual melting transition [3,13]. The profiles taken from x-ray Bragg peaks evolve continuously from a power law to a Lorentzian form, suggesting a second order transition at T_m = 100.25 ± 0.10°C. With regard to the electron diffraction pattern near T_m, Fig. 2c shows both a general increase in the diffuse scattering and the formation of a sharp ring with q vector corresponding to the superlattice spots in Fig. 2b, suggestive of anisotropic melting as discussed below.

In most anisotropic systems, the ratio of the correlation lengths along the principal axes remains constant during the melting transition. However for the Br_2 intercalant fluid, the length ratio in the 7-fold and $\sqrt{3}$-fold

directions evolves from ~3 very near T_m to < 1 at a temperature 0.4 K above T_m. In addition, the Br(2,0,0) peak, which involves contributions from both the Br_2 and the graphite, exhibits no measurable change through T_m; for melting into a 2D fluid, this peak should have exhibited a dramatic decrease in intensity (by ~75 %). This suggests that in the fluid phase substantial order has been maintained in the $\sqrt{3}$-direction in agreement with the electron diffraction results. Further study of the Br_2 melting is necessary before a direct comparison can be made to current theories [16] of the melting of a 2D anisotropic solid.

RESULTS FOR KHg_x-GIC

We have synthesized stages 1-3 KHg_x-GIC [5,17]. The KHg intercalant in the stage 1 compounds orders in the basal plane in a registered (2 x 2)R0° hexagonal network [18]. An additional symmetry corresponding to an ($\alpha\beta\gamma\delta$) interplanar correlation of the intercalate layers has been proposed by El Makrini based on room temperature x-ray powder patterns.[19] Subsequent to the discovery by Lagrange [18] of the (2 x 2) superlattice, other commensurate basal plane superlattice structures were observed in stage 1 KHg-GIC, e.g. ($\sqrt{3}$ x $\sqrt{3}$)R30° and (rectangular) ($\sqrt{3}$ x 2)R(30°,0°) [5,17]. The dominance of a particular superlattice was found to be strongly dependent on the sample preparation conditions.

During intercalation we have examined the temperature dependence of the (hk0) Bragg reflections using high resolution x-ray scattering. Changes in the basal plane and stacking order are reflected in the position and intensities of the (hk0) reflections. We have observed variations in the integrated intensity of the Bragg reflections indicative of high temperature phase transitions at 230 and 313°C. The change in intensity was hysteretic.

The room temperature basal plane coherence length estimated from the half-width of the (112) superlattice peak (uniquely identified with the intercalant lattice) exceeds 500 Å (spectrometer resolution). This observation is consistent with high resolution electron microscopy results where the intercalant lattice was directly imaged [5]. The direct image illustrated in Fig. 5 of the c-axis superlattice in a stage 1 KHg-intercalated kish graphite sample shows a well-ordered structure with long dislocation free regions (~ 100 Å x ~500 Å).

The dynamics associated with the intercalation process in the stage 1 compound were investigated in situ using (00ℓ) x-ray diffraction. The results indicate that the system first intercalates as stage 1 K-GIC (see Fig. 6), with a c-axis repeat distance, I_c = 5.35 Å (characteristic of stage 1 K-GIC) [1]. We infer (as first suggested by Lagrange [18]) that subsequent diffusion of mercury into the compound accounts for the increase in I_c to 10.2 Å. Low angle grain boundaries observed in the a-faces with electron microscopy [5] presumably facilitate the Hg diffusion.

ACKNOWLEDGMENTS

We wish to thank Dr. H. Suematsu for providing us with Kish graphite single crystals and Drs. G. Dresselhaus and P.M. Horn for helpful discussions. Support was provided by JSEP contract #DAAG-29-80-C-D104 (ARK and RJB) and AFOSR contract #F49620-83-C-0011 (AE, GT and MSD).

REFERENCES

1. For an extensive review, see M.S. Dresselhaus and G. Dresselhaus, Adv. Phys. 30, 139 (1981).
2. A.R. Kortan, A. Erbil, R.J. Birgeneau and M.S. Dresselhaus, Phys. Rev. Lett. 49, 1427 (1982).
3. A. Erbil, A.R. Kortan, R.J. Birgeneau, and M.S. Dresselhaus, in Intercalated Graphite, edited by M.S. Dresselhaus, G. Dresselhaus, J.E. Fischer, and M.J. Moran, Elsevier, New York, 1983, Materials Research Society Symposia Proceedings, vol. 20, p. 21.
4. Y. Iye, in Intercalated Graphite, edited by M.S. Dresselhaus, G. Dresselhaus, J.E. Fischer, and M.J. Moran, Elsevier, New York, 1983, Materials Research Society Symposia Proceedings, vol. 20, p. 185.
5. G. Timp, B.S. Elman, M.S. Dresselhaus and P. Tedrow, in Intercalated Graphite, edited by M.S. Dresselhaus, G. Dresselhaus, J.E. Fischer, and M.J. Moran, Elsevier, New York, 1983, Materials Research Society Symposia Proceedings, vol. 20, p. 201.
6. W.T. Eeles and J.A. Turnbull, Proc. Roy. Soc., London, Ser. A283, 179 (1965).
7. D. Ghosh and D.D.L. Chung, in Intercalated Graphite, edited by M.S. Dresselhaus, G. Dresselhaus, J.E. Fischer, and M.J. Moran, Elsevier, New York, 1983, Materials Research Society Symposia Proceedings, vol. 20, p. 15.
8. R. Moret, R. Comes, G. Furdin, H. Fuzellier and F. Rousseaux, in Intercalated Graphite, edited by M.S. Dresselhaus, G. Dresselhaus, J.E. Fischer, and M.J. Moran, Elsevier, New York, 1983, Materials Research Society Symposia Proceedings, vol. 20, p. 27.

9. G.S. Parry and D.E. Nixon, Nature, London, 216, 909 (1967); G.S. Parry, D.E. Nixon, K.M. Lester and B.C. Levene, J. Phys. C 2, 2156 (1969).

10. H. Zabel, S.C. Moss, N. Caswell and S.A. Solin, Phys. Rev. Lett. 43, 2022 (1979).

11. J.B. Hastings, W.D. Ellenson and J.E. Fischer, Phys. Rev. Lett. 42, 1552 (1979).

12. C.H. Olk, V. Yeh, F.J. Holler and P.C. Eklund, in Intercalated Graphite, edited by M.S. Dresselhaus, G. Dresselhaus, J.E. Fischer, and M.J. Moran, Elsevier, New York, 1983, Materials Research Society Symposia Proceedings, vol. 20, p. 259.

13. A. Erbil, 1983. Ph.D. Thesis, M.I.T., Cambridge, MA (unpublished).

14. V.L. Pokrovsky and A.L. Talapov, Phys. Rev. Lett. 42, 65 (1979); V.L. Pokrovsky and A.L. Talapov, Soviet. Phys. JETP 51, 134(1980).

15. A. Erbil, G. Dresselhaus and M. S. Dresselhaus, Phys. Rev. B25, 5451 (1982).

16. S. Ostlund and B.I. Halperin, Phys. Rev. B23, 335 (1981).

17. G. Timp, B.S. Elman, R. Al-Jishi, and G. Dresselhaus, Solid State Commun. 44, 987 (1982).

18. P. Lagrange, M. El Makrini, D. Guerard and A. Herold, Synth. Met. 2, 191 (1980).

19. M. El Makrini, 1982, Ph.D. Thesis, Univ. of Nancy, (unpublished).

Figure Captions

Fig. 1. The rectangular in-plane intercalate Br_2 unit cell (dashed lines) and the atomic arrangement in the extended lattice superimposed on the graphite lattice. Dashed-dotted lines show the primitive unit cell. The lengths $\sqrt{3}\ a_o$ = 4.26 Å and $7\ a_o$ = 17.22 Å are indicated.

Fig. 2. (a) Electron diffraction pattern at room temperature (298 K) from a single domain of a residue Br_2-GIC sample showing a ($\sqrt{3}$ x 7) superlattice. As the temperature increases through T_C a double diffraction pattern along the 7-fold direction is identified, as shown in (b) where T = 345 K. As the temperature is further increased to the vicinity of T_m, the superlattice spot pattern gives rise to a ring as shown in (c) at 372 K.

Fig. 3. X-ray intensity scans through the Br(0,6,0) peak position taken at various times after the introduction of Br_2 gas. The lines represent Gaussian functions with values of the width σ fit to the experimental points.

Fig. 4. The integrated intensity of the Br(0,6,0) peak as a function of time during the intercalation process.

Fig. 5. (00ℓ) lattice fringes from a stage 1 KHg_x-intercalated kish graphite sample.

Fig. 6. Integrated intensity of various diffraction peaks observed during the intercalation of KHg_x.

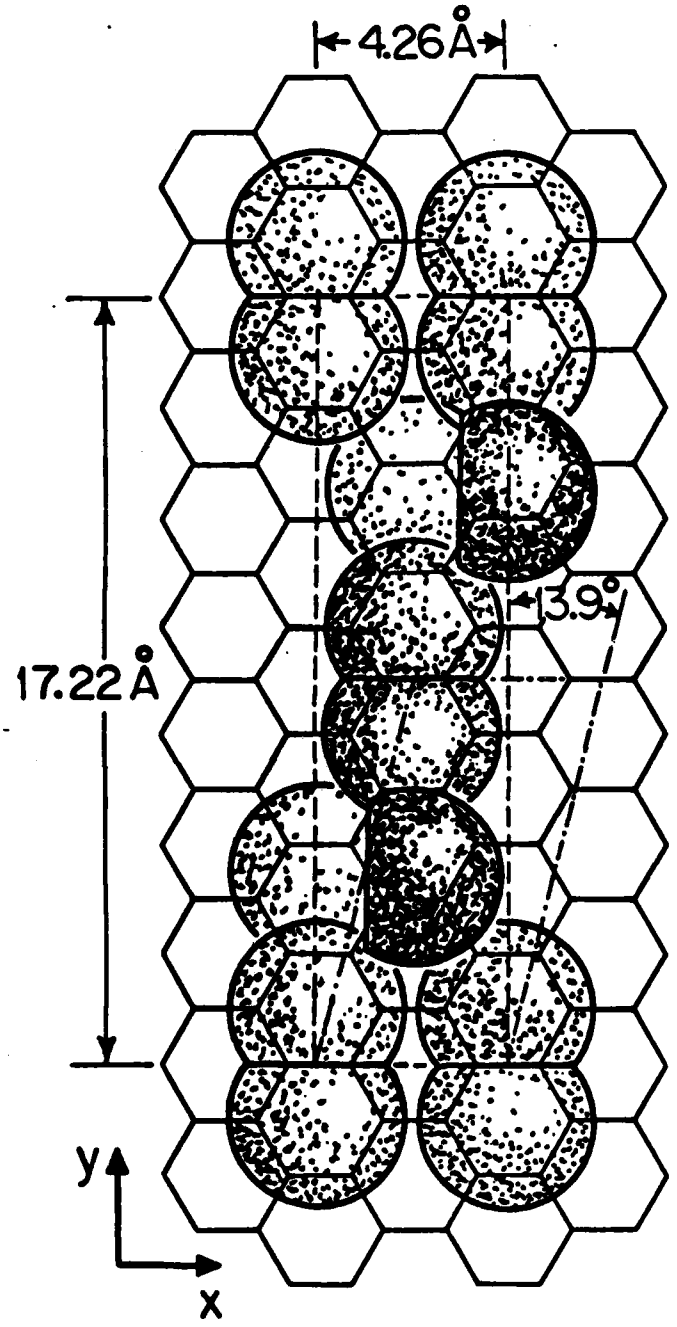

Fig. 1

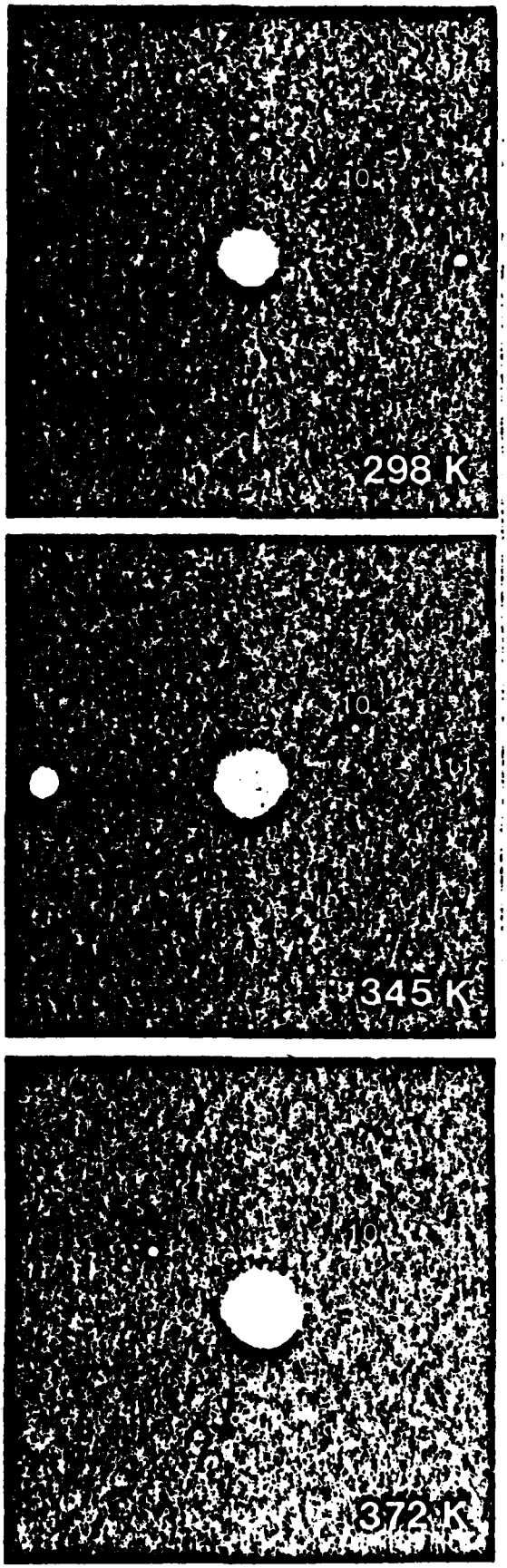

Fig. 2

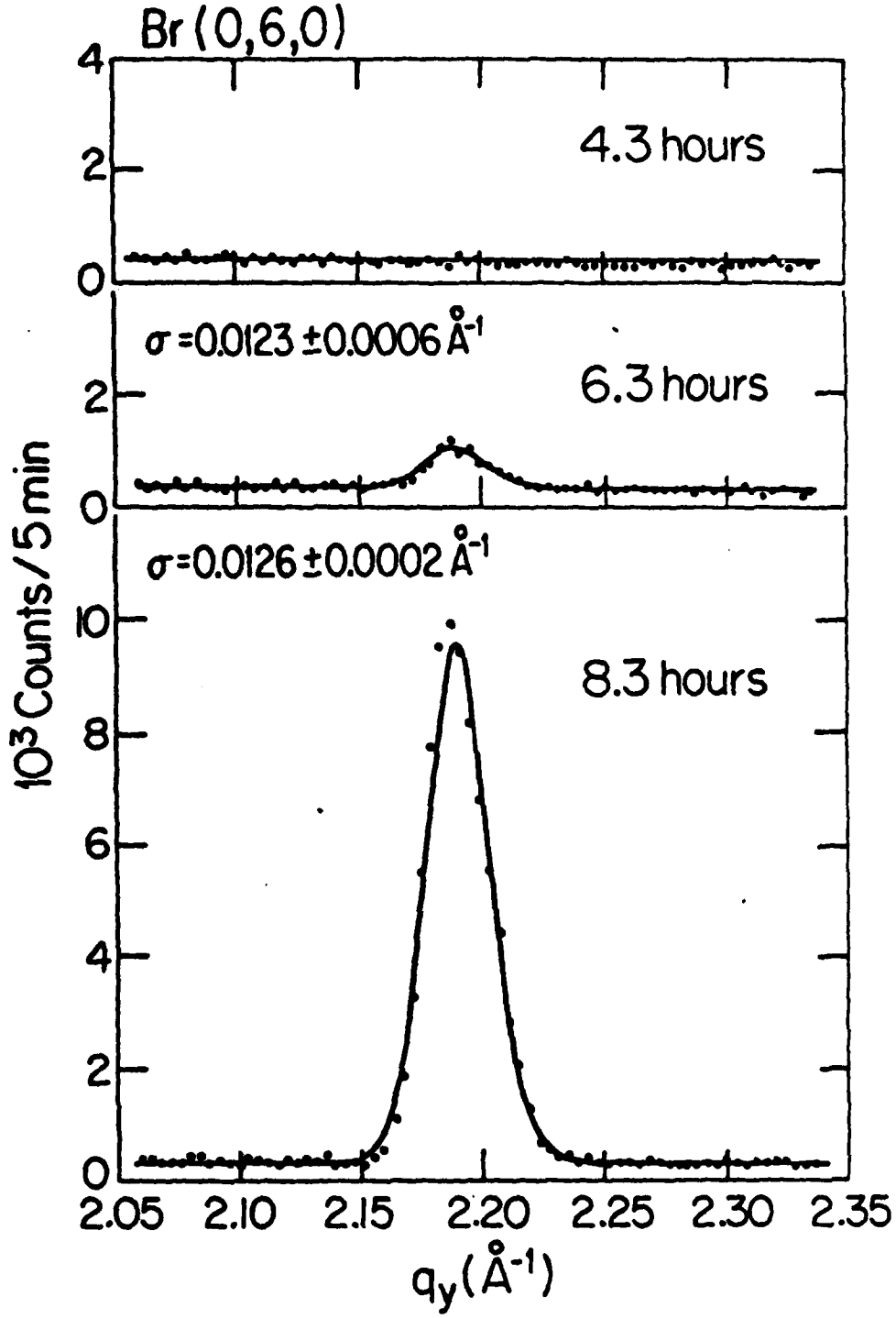
Br (0,6,0)
4.3 hours
σ =0.0123 ±0.0006 Å-1
6.3 hours
σ=0.0126 ±0.0002 Å-1
8.3 hours
10³ Counts/5 min
0
2
4
6
8
10
2.05
2.10
2.15
2.20
2.25
2.30
2.35
qy (Å-1)

Fig. 3

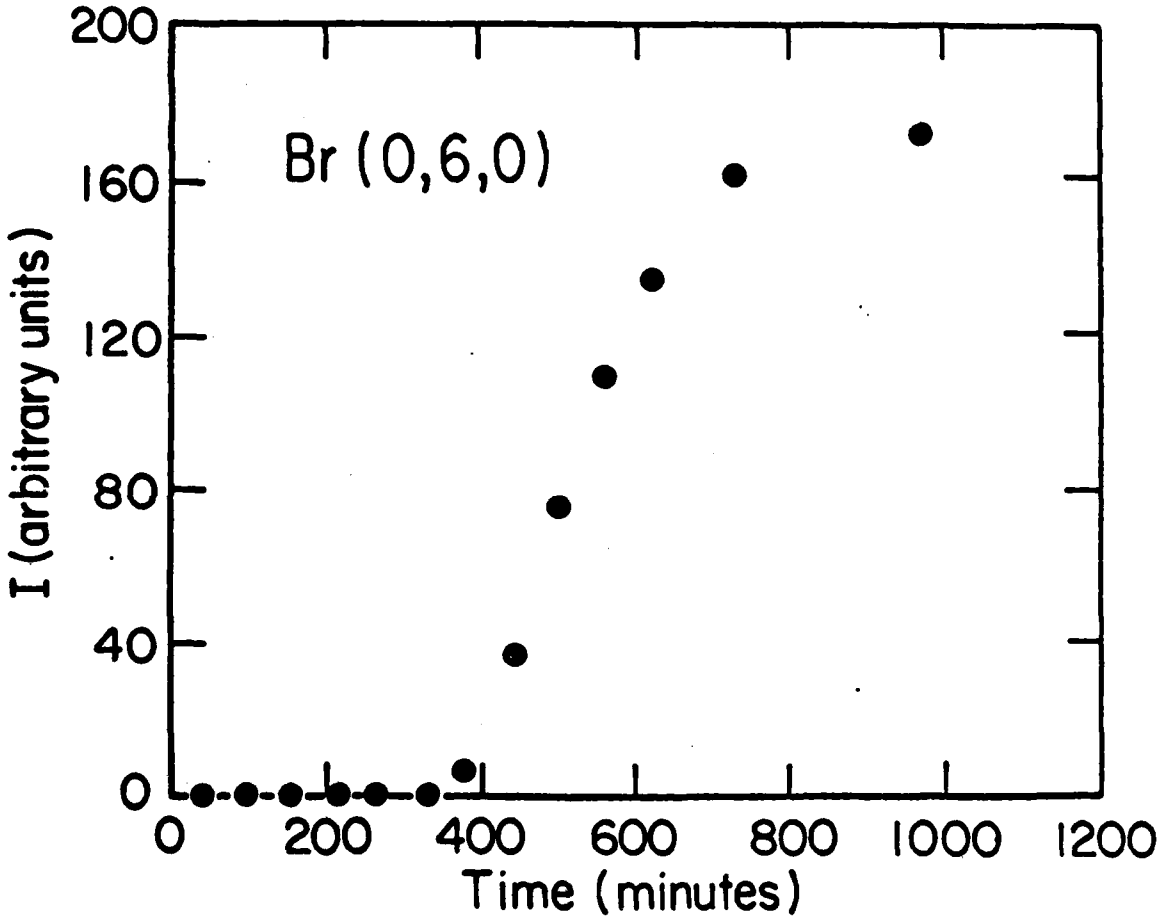
Br (0,6,0)
I (arbitrary units)
Time (minutes)
0
40
80
120
160
200
0
200
400
600
800
1000
1200

Fig. 4

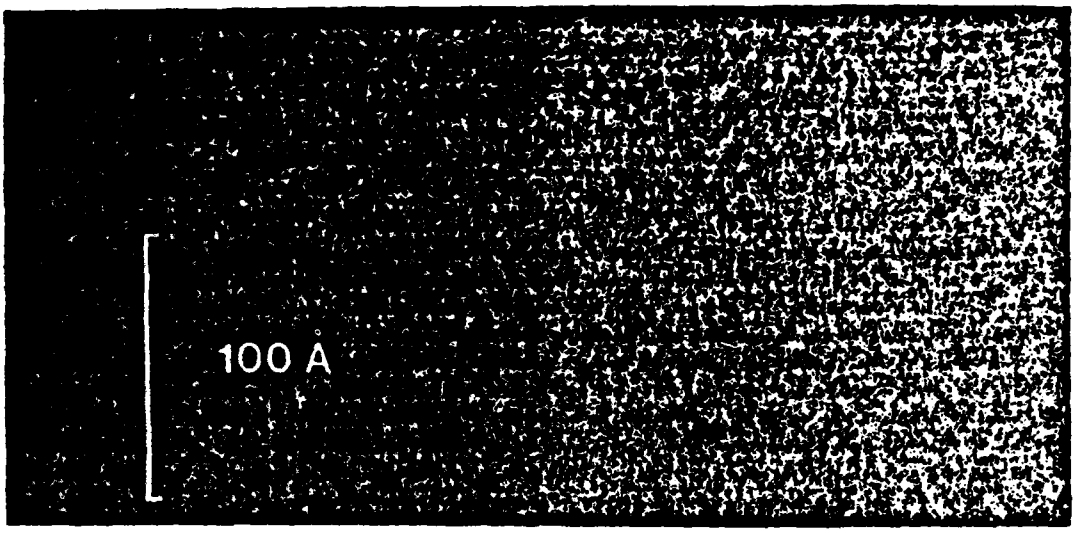

Fig. 5

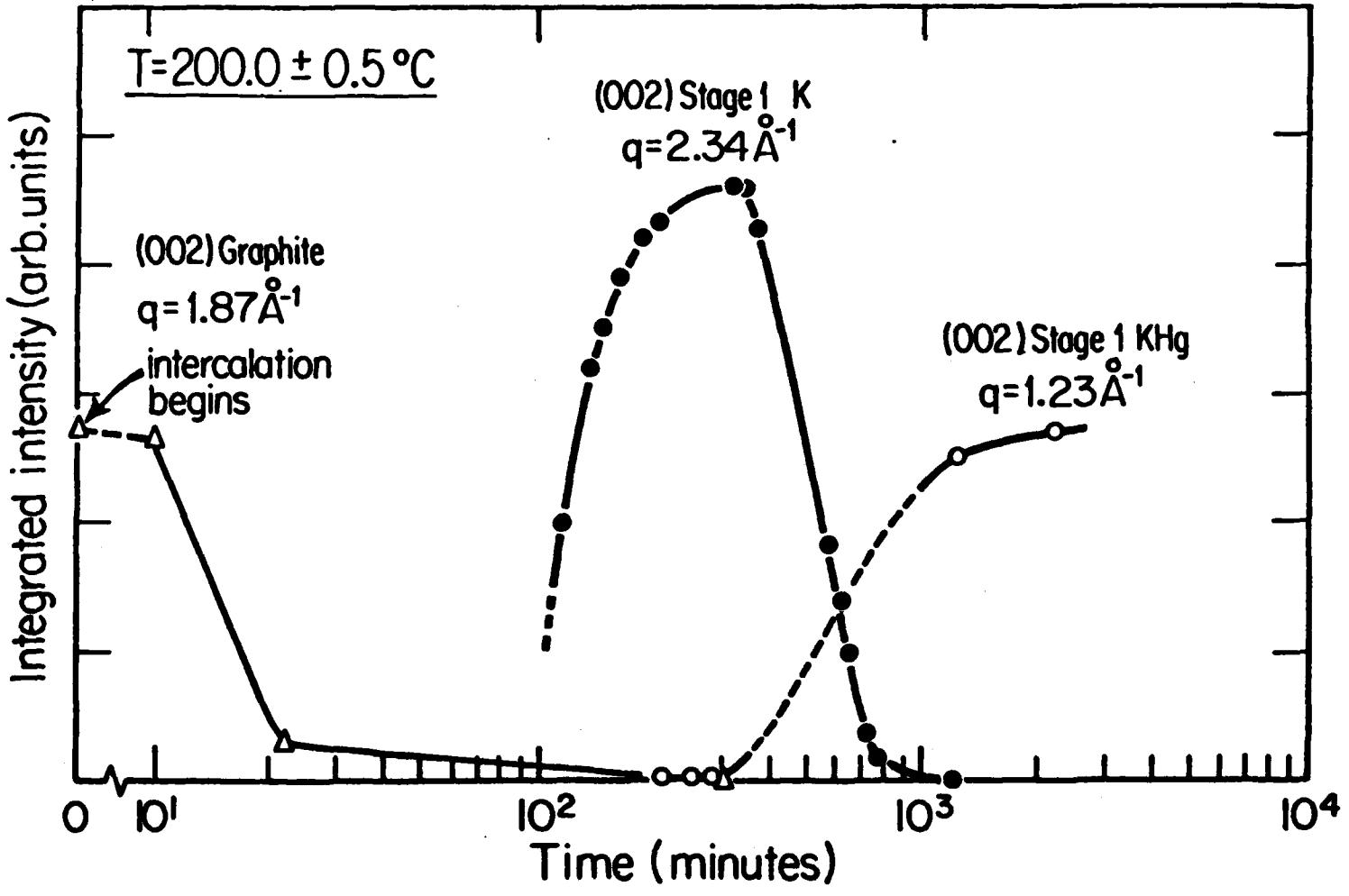
T=200.0 ± 0.5 °C
(002) Stage 1 K
q=2.34 Å-1
(002) Graphite
q=1.87 Å-1
intercalation
begins
(002) Stage 1 KHg
q=1.23 Å-1
Integrated intensity (arb.units)
0
10¹
10²
10³
10⁴
Time (minutes)

Fig. 6

END

FILMED

11-83

DTIC